# Mechanisms of Hydride Abstractions by Quinones

Xingwei Guo, Hendrik Zipse, and Herbert Mayr*

Department Chemie, Ludwig-Maximilians-Universität München, Butenandtstraße 5-13 (Haus F), 81377 München, Germany

S *Supporting Information*

ABSTRACT: The kinetics of the hydride abstractions by 2,3-dichloro-5,6-dicyano-*p*-benzoquinone (DDQ) from 13 C–H hydride donors (acyclic 1,4-dienes, cyclohexa-1,4-dienes, dihydropyridines), tributylstannane, triphenylstannane, and five borane complexes (amine–boranes, carbene–boranes) have been studied photometrically in dichloromethane solution at 20 °C. Analysis of the resulting second-order rate constants by the correlation $\log k_2(20\ °C) = s_N(E + N)$ (*J. Am. Chem. Soc.* **2001**, *123*, 9500) showed that the hydride abstractions from the C–H donors on one side and the Sn–H and B–H hydride donors on the other follow separate correlations, indicating different mechanisms for the two reaction series. The interpretation that the C–H donors transfer hydrogen to the carbonyl oxygen of DDQ while Sn–H and B–H hydride donors transfer hydride to a cyano-substituted carbon of DDQ is supported by quantum-chemical intrinsic reaction coordinate calculations and isotope labeling experiments of the reactions of D_8-cyclohexa-1,4-diene, Bu_3SnD, and pyridine·BD_3 with 2,5-dichloro-*p*-benzoquinone. The second-order rate constants of the reactions of tributylstannane with different quinones correlate linearly with the electrophilicity parameters *E* of the quinones, which have previously been derived from the reactions of quinones with π-nucleophiles. The fact that the reactions of Bu_3SnH with quinones and benzhydrylium ions are on the same $\log k_2$ vs *E* (electrophilicity) correlation shows that both reaction series proceed by the same mechanism and illustrates the general significance of the reactivity parameters *E*, *N*, and s_N for predicting rates of polar organic reactions.
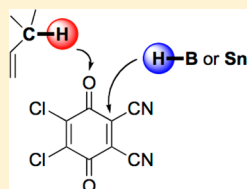
INTRODUCTION

Quinones belong to the most important oxidizing reagents in organic chemistry[1] and play an important role as hydrogen acceptors in biological processes.[2] However, mechanistic details of these processes are still discussed controversially.[3] Detailed studies by Linstead, Jackman, and co-workers[4] came to the conclusion that the oxidations of hydrocarbons by quinones usually occur via rate-determining hydride transfer, leading to delocalized carbocations, which rapidly lose a proton or are trapped by a nucleophile in a subsequent step. While this view was supported by Heesing et al.,[3h,i] Rüchardt et al. proposed a mechanism in which an initial hydrogen atom transfer leads to the formation of radicals.[3l] This view was supported by spin trapping of the intermediary radicals by nitrosobenzene.[3m,n] Chan and Radom pointed out, however, that the detection of a trapping product with nitrosobenzene cannot be considered as a proof for the operation of the radical mechanism.[3o] In a detailed computational investigation, they demonstrated that the course of the reaction depends on the solvent and that, in the reaction of 2,3-dichloro-5,6-dicyano-*p*-benzoquinone (DDQ; **1a**) with cyclohexa-1,4-diene, a radical mechanism proceeds in the gas phase and in heptane solution, whereas an ionic process with initial hydride transfer dominates in acetone and acetonitrile.[3o]

As depicted in Scheme 1, several mechanistic pathways are conceivable, e.g., (a) initial single electron transfer (SET), followed by hydrogen atom transfer (HAT), (b) initial hydrogen atom transfer, followed by an electron transfer, (c) one-step hydride transfer via O attack, and (d) one-step hydride transfer via C attack.

**Scheme 1. Possible Hydride Transfer Mechanisms of Quinones**
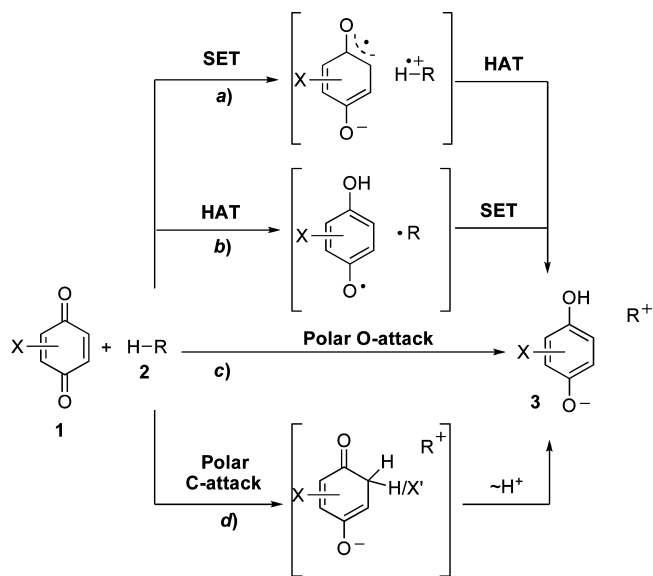
Among quinones, DDQ (**1a**) is the most frequently used hydride acceptor for oxidations of hydrocarbons[6] and dehydrogenative cross-coupling reactions.[7] We have previously demonstrated that the reactions of DDQ (**1a**) and of the

quinones **1b–f** (Scheme 2) with π-nucleophiles and amines most often proceed by polar pathways,[5] the rates of which can

Scheme 2. Quinones Investigated in This Work and Their Electrophilicity Parameters E (from Ref 5)
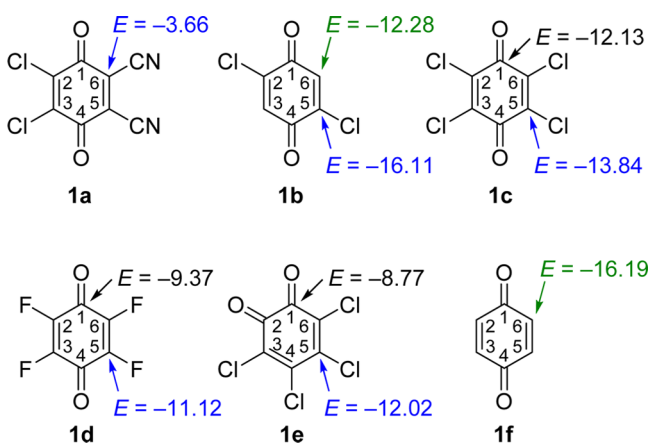
be described by eq 1,[8] which was developed to predict rates and selectivities of polar reactions.

$$\log k (20\ ^{\circ}\text{C}) = s_N(E + N) \tag{1}$$

In eq 1 the second-order rate constants ($\log k$) are described by two solvent-dependent, nucleophile-specific parameters (s_N, N) and one electrophile-specific parameter (E). Using a series of benzhydrylium ions and structurally related quinone methides as reference electrophiles, comprehensive nucleophilicity scales[9] have been established for different types of nucleophiles, including a variety of hydride donors.[10]

We now will report how eq 1 and the previously determined electrophilicity parameters E of the quinones **1a–f** (Scheme 2) can be employed to elucidate the mechanisms of hydrogen abstractions from structurally diverse hydride donors, as the allylic and benzylic C–H hydride donors **2a–l**, the tin hydrides **2n,o**, and the boron hydrides **2p–t** (Table 1).

RESULTS AND DISCUSSION

Kinetic Studies. Most kinetic investigations of the reactions of DDQ (**1a**) with the hydride donors **2** were performed in CH₂Cl₂ solution at 20 °C, and for some reactions of DDQ, solvent effects were investigated. CH₃CN and CD₃CN were employed as solvents for the kinetic investigations of the reactions of Bu₃SnH (**2n**) with **1b–f**. Most reactions were monitored by UV–vis spectroscopy at or close to the absorption maxima of the quinones (DDQ (**1a**), 286 or 390 nm; 2,5-dichloro-p-benzoquinone (**1b**), 275 nm; p-chloranil (**1c**), 290 nm; tetrafluoro-p-benzoquinone (**1d**), 256 nm; o-chloranil (**1e**), 457 nm). When acetone was used as a solvent, the formation of the hydroquinone DDQH₂ was monitored at 350 nm, because the absorption of the solvent covered that of the quinone. In all runs, at least 10 equiv of hydride donors was used to achieve pseudo-first-order kinetics; the rate constants were obtained by least-squares fitting of the monoexponential functions $A_t = A_0\, e^{-k_{obs}t} + C$ (for decrease) or $A_t = A_0 (1 - e^{-k_{obs}t}) + C$ (for increase) to the observed absorbances (Figure 1). ¹H NMR spectroscopy was employed to study the slow reaction of tributylstannane (**2n**) with p-benzoquinone (**1f**), which was used in excess over **2n**. The second-order rate constants k_2 given in Table 1 were derived from the slopes of
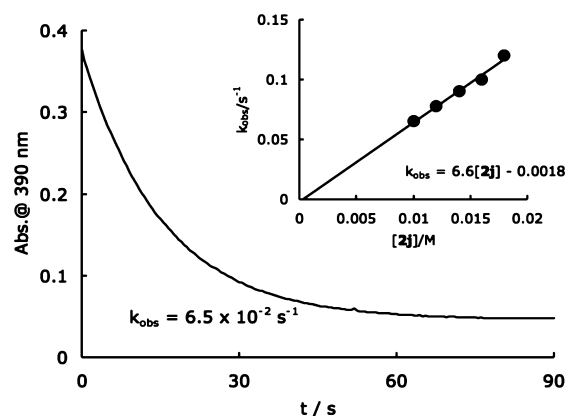

Figure 1. UV–vis spectroscopic monitoring of the reaction of DDQ ($c_0 = 1.0 \times 10^{-3}$ mol L⁻¹) with **2j** ($c_0 = 1.0 \times 10^{-2}$ mol L⁻¹) at 390 nm in CH₂Cl₂ at 20 °C. Inset: determination of the second-order rate constant $k_2 = 6.6$ L mol⁻¹ s⁻¹ from the dependence of the first-order rate constant k_{obs} on the concentration of **2j**.
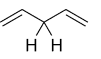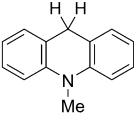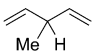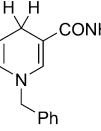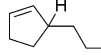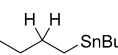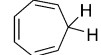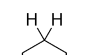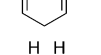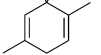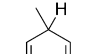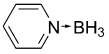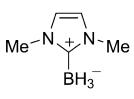
the correlations between the first-order rate constants k_{obs} and the concentrations of the hydride donors, which were linear with negligible intercepts (Figure 1, inset).

Correlation Analysis. In previous work we have determined the electrophilicity parameter of DDQ ($E = -3.66$ at C-5 or C-6) from the rates of its reactions with π-nucleophiles.[5a] By insertion of this electrophilicity parameter and the previously reported N and s_N parameters for the hydride donors **2** (Table 1) into eq 1, one obtains the calculated rate constants k_{cal} for hydride transfer to C-5 of DDQ, which are also given in Table 1. The last column of Table 1 shows that all C–H hydride donors investigated (**2a–m**) react 2–5 orders of magnitude faster than calculated, while the tin hydrides **2n,o** and the borane complexes **2p–t** react 1–2 orders of magnitude slower than calculated. This situation is illustrated in Figure 2 by the plot of $(\log k)/s_N$ against the nucleophilicity parameters N of hydride donors. One can see a fair linear correlation line ($r^2 = 0.91$) for the C–H hydride donors which is 3–4 units higher than the calculated correlation line and a second correlation for B–H or Sn–H hydride donors which is slightly below the calculated correlation line but still is within the confidence limits of eq 1. Two different mechanisms are thus indicated.

As the nucleophile-specific parameters N and s_N of eq 1 have been derived from the reactivities of various types of nucleophiles toward C electrophiles (benzhydrylium ions and quinone methides) and the electrophilicity parameters E have been derived from reactions of various electrophiles with C nucleophiles, eq 1 should only hold for reactions where a new C–X bond (X = C, H, heteroatom) is formed in the rate-determining step. Thus, eq 1 should be applicable to mechanism d of Scheme 1 (polar hydride transfer to C) but not to mechanism c (polar hydride transfer to O). Subsequently, we wi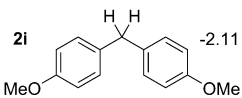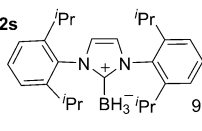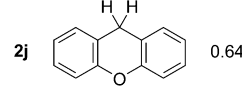ll show that the reactions of the B–H and Sn–H hydride donors actually follow mechanism d with rate constants close to those predicted by eq 1, while C–H hydride donors transfer H⁻ to the carbonyl oxygen much faster than calculated by eq 1.

As tributylstannane (**2n**) reacted 300 times faster with DDQ than triphenylstannane (**2o**), we excluded rate-determining hydrogen atom transfer for these reactions (mechanism b, Scheme 1), because Ingold reported that homolytic Sn–H cleavage is faster in Ph₃SnH than in Bu₃SnH.[11]

Table 1. Experimental Rate Constants of the Reactions of DDQ (1a) with the Reducing Agents 2a–t in CH$_2$Cl$_2$ at 20 °C and Calculated Rate Constants for C Attack from Eq 1 by Using the Electrophilicity Parameter of E(1a) = −3.66 (from Ref 5a)

H-donor	N (s_N)[a]	k_2 / M^{-1}s^{-1}	k_{cal} / M^{-1}s^{-1}	log(k_2/k_{cal})	H-donor	N (s_N)[a]	k_2 / M^{-1}s^{-1}	k_{cal} / M^{-1}s^{-1}	log(k_2/k_{cal})
2a	−2.99 (0.97)	5.2 × 10^{-4} [b]	3.5 × 10^{-7}	3.2	2k	5.54 (0.90)	>10^{7} [j]	49	>5
2b	−3.08 (0.97)	2.2 × 10^{-3} [c]	2.9 × 10^{-7}	3.9	2l	8.67 (0.82)	>10^{7} [k]	1.3 × 10^{4}	>3
2c	−0.88 (0.94)	7.5 × 10^{-3}	5.4 × 10^{-5}	2.1	2m	−0.30 (1.07)	6.2 × 10^{-2}	5.8 × 10^{-5}	3.0
2d	0.52 (0.97)	2.2 [d]	9.0 × 10^{-4}	3.4	2n	9.96 (0.55)	6.2 × 10^{2}	2.9 × 10^{3}	−0.7
2e	0.09 (0.98)	0.49 [e]	3.2 × 10^{-4}	3.2	2o	5.64 (0.59)	2.1	15	−0.9
2f	1.88 (0.96) [f]	1.1 × 10^{2} [g]	2.0 × 10^{-2}	3.7	2p	7.97 (0.75)	3.1	1.7 × 10^{3}	−2.7
2g	4.95 (0.79) [f]	1.2 × 10^{3} [h]	10	2.1	2q	8.90 (0.75)	1.7 × 10^{2}	8.5 × 10^{3}	−1.7
2h	4.27 (0.86) [f]	5.9 × 10^{4}	3.3	4.3	2r	10.01 (0.75)	5.1 × 10^{3}	5.8 × 10^{4}	−1.1
2i	−2.11 (0.98) [f]	3.8 × 10^{-2}	2.2 × 10^{-6}	4.2	2s	9.55 (0.81)	2.9 × 10^{3}	5.9 × 10^{4}	−1.3
2j	0.64 (0.97)	6.6 [i]	1.2 × 10^{-3}	3.7	2t	11.88 (0.71)	1.7 × 10^{4}	6.9 × 10^{5}	−1.6

[a]From ref 10. [b]k_2 = 2.91 × 10^{-5} M^{-1} s^{-1} has been reported in AcOH at 25 °C.[3c] [c]k_2 = 1.22 × 10^{-4} M^{-1} s^{-1} has been reported in AcOH at 25 °C.[3c] [d]k_2 = 0.20 M^{-1} s^{-1} has been reported in AcOH at 25 °C.[3c] [e]k_2 = 5.4 × 10^{-2} M^{-1} s^{-1} has been reported in AcOH at 25 °C;[3c] k_2 = 1.3 × 10^{-2} M^{-1} s^{-1} has been reported in dioxane at 25 °C;[3i] k_2 = 7.8 × 10^{-3} M^{-1} s^{-1} (20 °C) in dioxane has been calculated from activation parameters given in ref 3n. [f]Determined in this work using our standard procedure (Supporting Information, pp S20−S24). As only two reference electrophiles of similar reactivity were employed, the splitting up of log k_2 into N and s_N has not been independently justified. [g]k_2 = 9.0 M^{-1} s^{-1} has been reported in AcOH at 25 °C.[3d] [h]k_2 = 61.4 M^{-1} s^{-1} has been reported in AcOH at 25 °C.[3d] [i]k_2 = 0.46 M^{-1} s^{-1} has been reported in CH$_3$CN at 25 °C.[3m] [j]k_2 = 1.5 × 10^{6} M^{-1} s^{-1} has been reported in CH$_3$CN at 25 °C.[3j] [k]k_2 = 8.3 × 10^{6} M^{-1} s^{-1} has been reported in CH$_3$CN at 25 °C.[3j]

Solvent and Kinetic Isotope Effects. Table 2 and Figure 3 show that the rates of hydride abstraction from cyclohexa-1,4-diene (**2e**) do not correlate with Reichardt's solvent polarity parameter E_T.[12] In contrast, the rate constants for the reactions of DDQ with Bu$_3$SnH (**2n**) increase linearly with E_T, while the hydride abstractions from pyridine−borane become slightly slower with increasing E_T.

The large solvent effect for the reaction of DDQ with tributylstannane (**2n**) indicates charge separation in the transition state, as shown in Figure 4, where C attack of **2n** on DDQ forms an ion pair, which can be stabilized by a polar solvent. From Hammond's postulate, we can expect a large solvent effect based on a late transition state (see also the quantum chemical calculations below). The slight decrease of the reaction rates with increasing solvent polarity in the corresponding reaction with the borane−pyridine complex **2r** can be attributed to the dipolar character of **2r** that is stabilized by a polar solvent.

In line with an earlier report on dehydrogenations of hydroaromatic compounds with quinones,[3e] large primary isotope effects of k_H/k_D = 5.8−9.0 were observed for the reactions of DDQ with cyclohexa-1,4-diene (Table 2). The small, solvent-dependent kinetic isotope effects which were observed for the corresponding reactions with tributylstannane (k_H/k_D = 0.94−2.2) and the borane−pyridine complex **2r** (k_H/k_D = 1.5−2.5) also have precedents in the literature.[13,14] As summarized by Wigfield et al.,[14b] the rather low and, in part even inverse, primary KIE data for borohydride reductions of ketones have qualitatively been rationalized with product-like transition states. This interpretation has also been supported by Yamataka and Hanafusa,[14c] whose calculations with quantitative transition state models document the possibility of very small primary H/D isotope effects in ketone reductions for very late (that is, product-like) transition states. That primary KIE values can actually become inverse for these reactions can be explained by the smaller stretching force constants of B−H and Sn−H in comparison to C−H bonds.
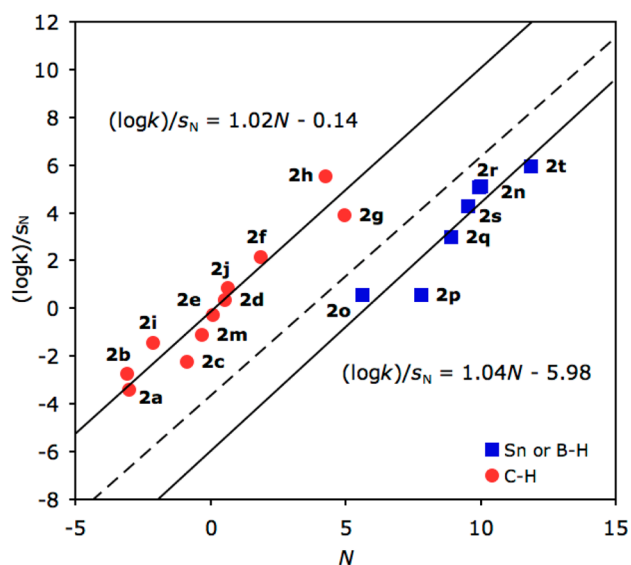
Figure 2. Correlations of $(\log k)/s_N$ vs N for the reactions of DDQ (**1a**) with hydride donors **2**. The broken line represents the calculated line according to eq 1 using the electrophilicity parameter $E = -3.66$, which was derived from reactions of DDQ with C nucleophiles, and the N/s_N parameters of the hydride donors, which were derived from their reactions with benzhydrylium ions.

Table 2. Solvent and Kinetic Isotope Effects for Reactions of DDQ (1a) with 2e,n,r (20 °C)

solvent	$E_T{}^a$	$k_H/M^{-1} s^{-1}$	$k_D/M^{-1} s^{-1}$	k_H/k_D
	DDQ + Cyclohexa-1,4-diene/D$_8$ (**2e**)			
cyclohexane	31.2	1.4×10^{-1}		
n-Bu$_2$O	32.0	4.6×10^{-2}	5.1×10^{-3}	9.0
THF	37.4	4.2×10^{-3}	7.3×10^{-4}	5.8
CH$_2$Cl$_2$	41.1	4.9×10^{-1}	6.8×10^{-2}	7.2
acetone	42.2	1.2×10^{-2}		
CH$_3$CN	46.0	6.2×10^{-2}	9.7×10^{-3}	6.4
	DDQ + Bu$_3$SnH/D (**2n**)			
cyclohexane	31.2	1.5×10^1	1.6×10^1	0.94
n-Bu$_2$O	32.0	2.5×10^1	1.4×10^1	1.8
THF	37.4	4.8×10^1	3.7×10^1	1.3
CH$_2$Cl$_2$	41.1	6.2×10^2	3.7×10^2	1.7
acetone	42.2	3.6×10^2	2.7×10^2	1.3
CH$_3$CN	46.0	6.0×10^3	2.7×10^3	2.2
	DDQ + pyridine·BH$_3$/D$_3$ (**2r**)			
cyclohexane	31.2	3.0×10^4	1.3×10^4	2.3
n-Bu$_2$O	32.0	6.4×10^3	4.2×10^3	1.5
THF	37.4	5.4×10^2	2.2×10^2	2.5
CH$_2$Cl$_2$	41.1	5.1×10^3	2.8×10^3	1.8
acetone	42.2	1.7×10^3	7.9×10^2	2.2
CH$_3$CN	46.0	2.2×10^3	1.0×10^3	2.2

^{a}From ref 12.

Reactions of Tributylstannane with Different Oxidants. Table 3 and Figure 5 show that the rate constants (log k_2) for the reactions of Bu$_3$SnH with quinones and benzhydrylium ions follow a common correlation with the electrophilicity parameters of quinones and benzhydrylium ions, which were derived from reactions with π-nucleophiles. As the reactions of stannanes with benzhydrylium ions have previously been shown to proceed by a polar mechanism,[10] the correlation in Figure 5 supports a polar reaction mechanism via
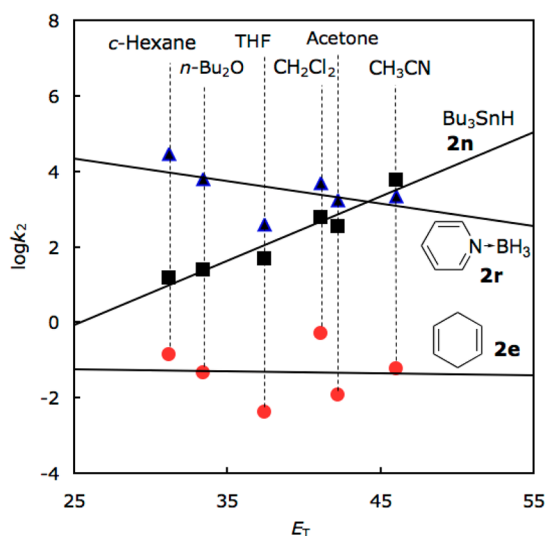

Figure 3. Solvent effects for the reactions of DDQ (**1a**) with **2e,n,r**.
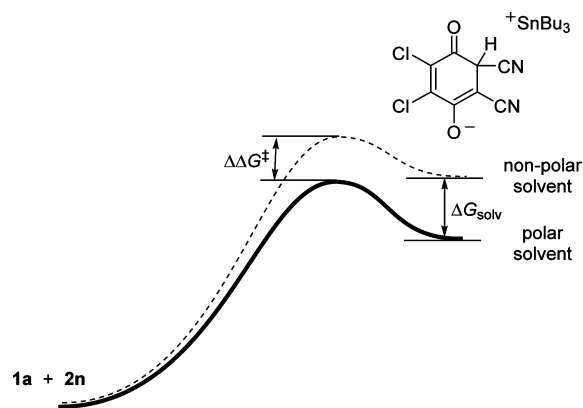

Figure 4. Solvent effect on the reaction of DDQ (**1a**) with tributylstannane (**2n**).

Table 3. Comparison of Rate Constants of the Reactions of Tributylstannane (2n) with Quinones in CH$_3$CN and Benzhydrylium Ions in CH$_2$Cl$_2$

electrophile^a	E	$k_2/M^{-1} s^{-1}$	$k_{calc}{}^b/M^{-1} s^{-1}$	$\log (k_2/k_{calc})$
(dpa)$_2$CH$^+$	−4.72	$7.2 \times 10^{2\,c}$	7.6×10^2	−0.03
(dma)$_2$CH$^+$	−7.02	$5.4 \times 10^{1\,c}$	4.1×10^1	0.12
(pyr)$_2$CH$^+$	−7.69	$1.7 \times 10^{1\,c}$	1.8×10^1	−0.02
(jul)$_2$CH$^+$	−9.45	1.8^c	1.9	−0.03
DDQ (**1a**)	−3.66	6.0×10^3	2.9×10^3	0.31
2,5-dichloro-p-benzoquinone (**1b**)	−12.28	2.5×10^{-2}	5.3×10^{-2}	−0.33
p-chloranil (**1c**)	−12.13	9.3×10^{-1}	6.4×10^{-2}	1.16
tetrafluoro-p-benzoquinone (**1d**)	−9.37	1.5	2.1	−0.15
o-chloranil (**1e**)	−8.77	3.0×10^2	4.5	1.82
p-benzoquinone (**1f**)	−16.19	9.4×10^{-5}	3.7×10^{-4}	−0.60

^{a}For structures see Figure 5. ^{b}Calculated by substituting $N = 9.96$ and $s_N = 0.55$ of Bu$_3$SnH (from ref 15) and the electrophilicities E of the reaction partners into eq 1. ^{c}From ref 15.

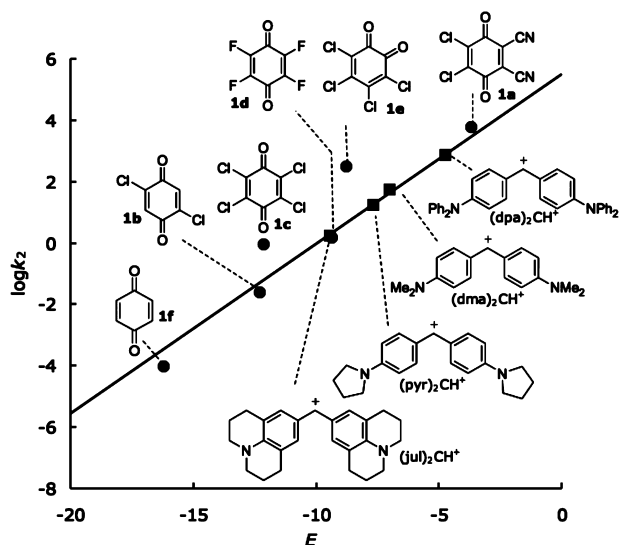C attack for the reactions of Sn−H hydride donors with quinones.

Figure 5. Correlation of log k_2 vs E for the reactions of Bu$_3$SnH (**2n**) with quinones (in MeCN) and benzhydrylium ions (in CH$_2$Cl$_2$). Data are taken from Table 3.

Deuterium labeling experiments with 2,5-dichlorobenzoquinone (**1b**) provide a further tool to differentiate between C and O attack of different hydride donors. When **1b** was treated with Bu$_3$SnD in CH$_2$Cl$_2$ at 20 °C, a ~1:1 mixture of the deuterated and nondeuterated hydroquinones **3-D** and **3-H** was isolated in 80% yield (Scheme 3). The formation of **3-D**, i.e., a product with deuterium at C-3, indicates a C attack pathway, e.g., via intermediates **4** and **5**.
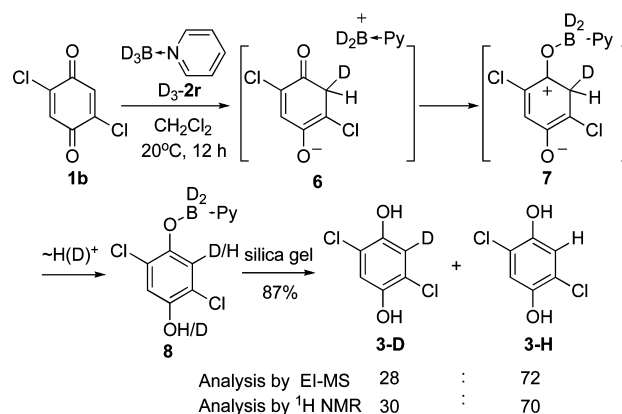
Scheme 3. Reaction of 2,5-Dichloro-*p*-benzoquinone (1b) with Bu$_3$SnD


| Analysis by EI-MS | 42 | : | 58 |
| Analysis by ^{1}H NMR | 49 | : | 51 |
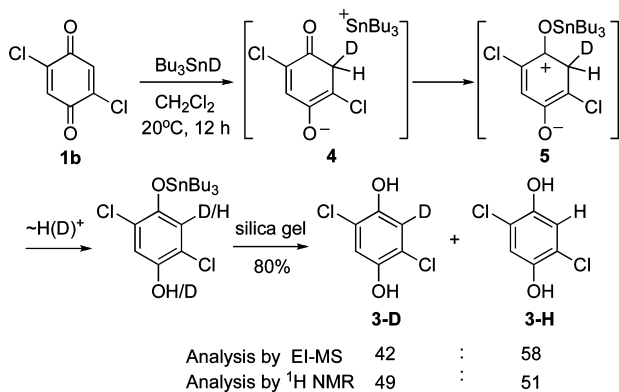
Similarly, when 2,5-dichlorobenzoquinone (**1b**) reacted with the deuterated borane pyridine complex **D$_3$-2r**, a 3:7 mixture of **3-D** and **3-H** was isolated in 87% yield (Scheme 4), which also supports a C attack pathway via intermediates **6** and **7**. The smaller ratio **3-D**/**3-H** may be due to the proton exchange of pyridine·BD$_3$ with the phenolic proton of **8**, as an earlier study showed that amine−borane complexes undergo a rapid proton−deuterium exchange with heavy water under acidic conditions.[16]

In contrast, only a trace amount of deuterium was found in the hydroquinone, which was obtained in 17% yield from the reaction of **1b** with perdeuterated cyclohexa-1,4-diene (**D$_8$-2e**) in CH$_2$Cl$_2$ at 20 °C after 48 h (Scheme 5).[17] While the E parameters for C attack at quinones cannot be applied to derive

Scheme 4. Reaction of 2,5-Dichlorobenzoquinone (1b) with the Pyridine−Borane Deuteride Complex (D$_3$-2r)

| Analysis by EI-MS | 28 | : | 72 |
| Analysis by ^{1}H NMR | 30 | : | 70 |

Scheme 5. Reaction of 2,5-Dichloro-*p*-benzoquinone (1b) with D$_8$-Cyclohexadiene (D$_8$-2e)

| Analysis by EI-MS | 3 | : | 97 |
| Analysis by ^{1}H NMR | 4 | : | 96 |
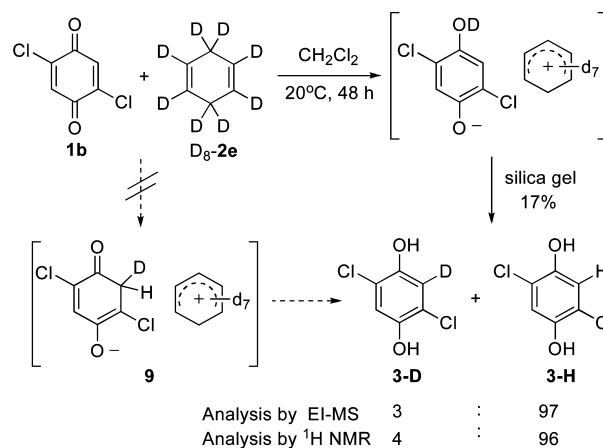
the rate of O attack, the formation of a small yield of **3** from **1b** and **D$_8$-2e** is surprising in view of the fact that a rate constant of 10^{-12} M^{-1} s^{-1} can be calculated for the formation of **9** by attack of cyclohexa-1,4-diene (**2e**) at the CH position of **1b**, which is far too small to explain the observed traces of **3-D**.

In order to examine the origin of **3-D**, O-deuterated 2,5-dichlorohydroquinone was prepared by deuterium exchange with heavy water and dissolved in CH$_2$Cl$_2$, the solvent used for the hydride transfer reaction. Scheme 6 shows that the exchange of deuterium at the C-3 position occurs slowly at 20 °C. The small amount (4%) of **3-D** observed after 48 h, therefore, suggests that the trace amount (3%) of **3-D** found in

Scheme 6. Examination of Deuterium Exchange at the Product Stage

t	relative abundance by GC/MS		
24 h	2	:	98
48 h	4	:	96
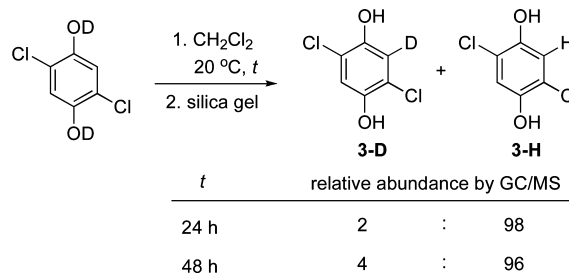
Figure 6. Free energy profile for the reaction of DDQ (**1a**) with cyclohexadiene (**2e**) (RM06-2X/def2-TZVPP//B97D/6-31+G(d,p)//PCM/UFF) in CH$_2$Cl$_2$ together with selected transition structures.

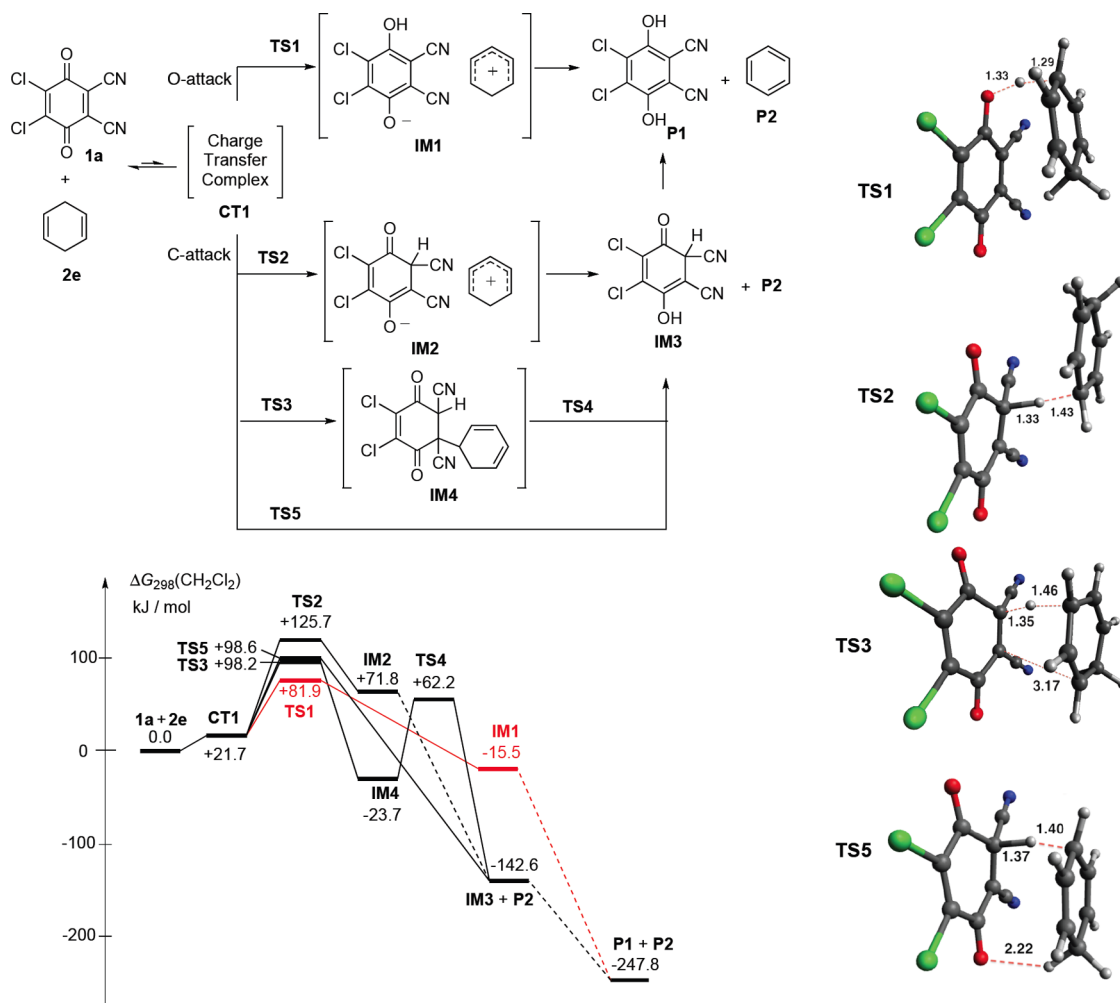the reaction of **1b** with C$_6$D$_8$ comes from deuterium exchange at the product stage and not from the intermediacy of **9**.

Computational Studies. DFT studies of the reactions of DDQ with cyclohexa-1,4-diene (**2e**), Me$_3$SnH (**2n′**), and trimethylamine−borane complex (**2p**) were performed using Gaussian 09.[18] The B97D functional was used in combination with the 6-31+G(d,p) basis set (LANL2DZ ECP for Sn atoms) for structure optimization and frequency calculations. Since Radom has shown that transition structures obtained in the presence of a solvent model may deviate significantly from the gas-phase structures,[3o] the PCM/UFF model for CH$_2$Cl$_2$ has been used for all geometry optimizations in this study. Geometries of the transition states were verified by vibrational frequency calculations. The nature of the most favorable transition states was further verified by IRC calculations (50 steps in each direction) and subsequent structure optimizations to the next local minimum energy structure. Thermal corrections were calculated from unscaled frequencies at 298.15 K and 1 atm. Refined electronic energies were obtained from single-point calculations on the B97D geometries using Truhlar's meta hybrid exchange-correlation functional M06-2X with the triple-ζ quality def2-TZVPP basis sets, again using the PCM/UFF model for CH$_2$Cl$_2$. All free energies in solution have been corrected to correspond to a standard state of 1 mol L^{-1}.[19] The stabilities of the restricted wave functions (RB97D

and RM06-2X) have been checked for all transition states. An ultrafine grid was used throughout this study for numerical integration of the density.

The energy profile as well as the optimized transition structures for the different modes of reaction of DDQ (**1a**) with cyclohexadiene (**2e**) are shown in Figure 6. The geometry of **TS1**, the most favorable pathway, closely resembles that previously calculated by Chan and Radom for polar solvents.[3o] The formation of the CT complex **CT1** between DDQ (**1a**) and **2e** is endergonic by 22 kJ mol^{-1}. From **CT1**, hydride transfer to O of DDQ via **TS1** requires an activation free energy of 60 kJ mol^{-1}, resulting in an overall barrier of 82 kJ mol^{-1}. Surprisingly, the generation of the ion pair intermediate **IM1** from DDQ (**1a**) and cyclohexa-1,4-diene (**2e**) is exergonic by 16 kJ mol^{-1}. Further stabilization by proton transfer and separation of the product complex gives the final products **P1** and **P2**.

The barrier for hydride transfer from **2e** to C-5 of DDQ via **TS2** is 44 kJ mol^{-1} higher than that for O attack, and the free energy of the generated ion pair intermediate **IM2** is 87 kJ mol^{-1} higher than that of **IM1**. In addition, the transition state of the ene reaction **TS3** is favored by 28 kJ mol^{-1} over **TS2**, and the formation of the ene adduct **IM4** is exergonic by 24 kJ mol^{-1}. Further elimination of benzene from **IM4** requires an activation free energy of 86 kJ mol^{-1} (for the structure of **TS4**
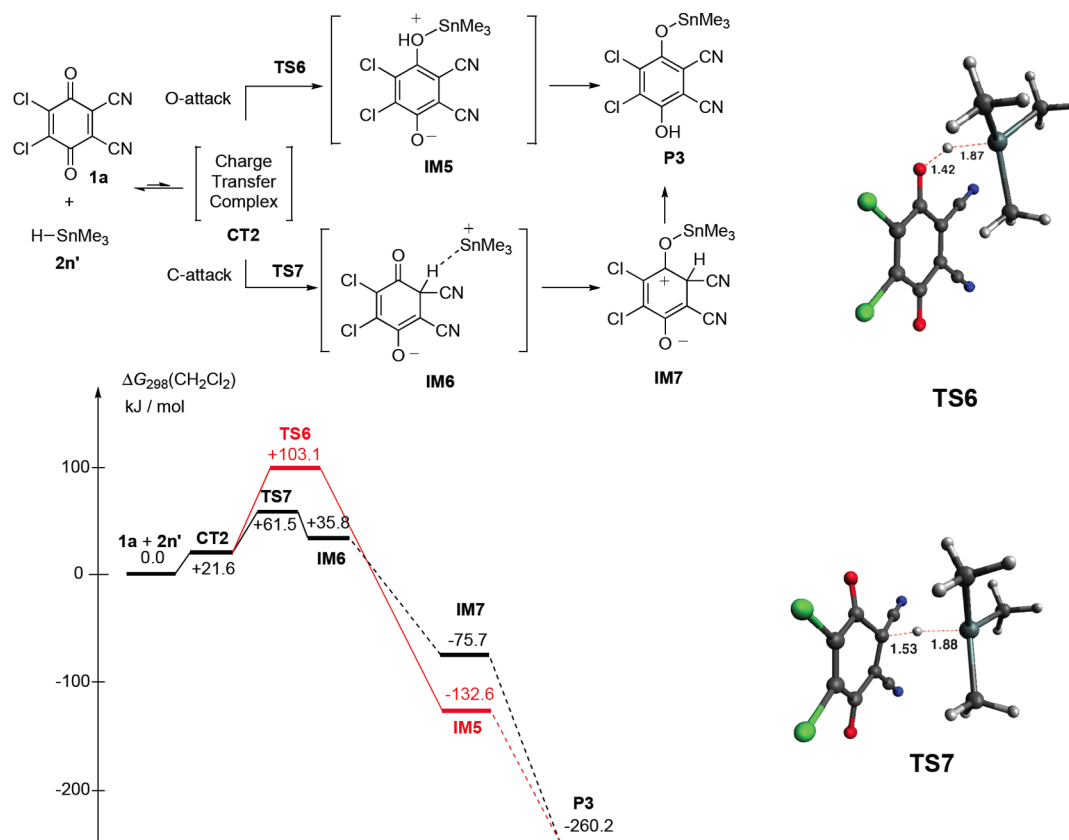
Figure 7. Free energy profile for the reaction of DDQ (**1a**) with trimethylstannane (**2n′**) (RM06-2X/def2-TZVPP//B97D/6-31+G(d,p)//PCM/UFF) in CH_2Cl_2 together with selected transition structures.

see the Supporting Information, p S50). Interestingly, concerted transfer of two hydrogen atoms via **TS5** faces a reaction barrier (99 kJ mol^{-1}) comparable to that of the stepwise process through **TS3** and **IM4**. The restricted wave functions were examined to be stable for the structures in Figure 6, which indicates that these stationary points are not of biradical type. The charge distributions in these structures further confirm the polar character of these pathways (see the Supporting Information, pp S35−S36).

Figure 7 shows the free energy profiles of the two different reaction pathways for the reaction of DDQ (**1a**) with trimethylstannane (**2n′**), a model for the experimentally studied tributylstannane **2n**. The O-attack pathway, i.e., hydride transfer via **TS6**, requires an overall activation free energy of 103 kJ mol^{-1} to form the zwitterionic intermediate **IM5**. The formation of **IM5** from DDQ (**1a**) and **2n′** is exergonic by 133 kJ mol^{-1}, and a subsequent proton shift leads to the more stable final product **P3**. The competing hydride transfer to C-5 of DDQ (**1a**) via **TS7** is favored by 42 kJ mol^{-1} over the O-attack pathway. While the generation of the ion pair intermediate **IM6** from **1a** and **2n′** is endergonic by 36 kJ mol^{-1}, stabilization comes from the following migration of the SnMe$_3$ group to the adjacent oxygen atom and the subsequent proton transfer, which gives the final product **P3**. Though there seems to be a small barrier of ∼10 kJ mol^{-1}, the transition state for the migration of the SnMe$_3$ group could not be located due to the exceedingly flat potential energy surface.

As illustrated in Figure 8, the O- and C-attack pathways of the reaction of DDQ (**1a**) with trimethylamine−borane complex (**2p**) show a pattern similar to that of the reactions with trimethylstannane. C attack is favored over O attack by 47

kJ mol^{-1}. The formation of **IM9** is a highly endergonic process by 61 kJ mol^{-1}: i.e., **IM9** is only 8 kJ mol^{-1} more stable than the transition state **TS9**. As in the reaction with the stannane, the major stabilization comes through migration of boron to the oxygen.

The activation Gibbs free energies for C- and O-attack pathways of the reaction of DDQ (**1a**) with various hydride donors **2**, which were analogously calculated on the same level of theory (Supporting Information, Table S64) were converted into second-order rate constants by the Eyring equation. The numbers given in Table 4 include statistical corrections, considering the number of equivalent positions in the quinones and the hydride donors. As shown in Table 4, O attack is favored for all computationally examined C−H hydride donors,[20] while C attack is favored for all computationally examined B−H and Sn−H hydride donors, in agreement with the interpretation of our experimental observations. Efforts to rationalize the different behaviors of these two groups of hydride donors by analysis of transition state charge distribution or distortion/interaction energy analysis[21] (see the Supporting Information, pp S32−S34) have, unfortunately, not been successful. Obviously, there is not *one* dominant component which accounts for the variations of the barriers, and the different selectivities of C−H and Sn−H/B−H donors are not due to a single factor.[30]

As shown in Figure 9, the rate constants derived from quantum chemically calculated activation free energies for O attack of C−H hydride donors and for C attack of tin and boron hydrides correlate well with the experimental values, which demonstrates the consistency of the computational method employed in this work.
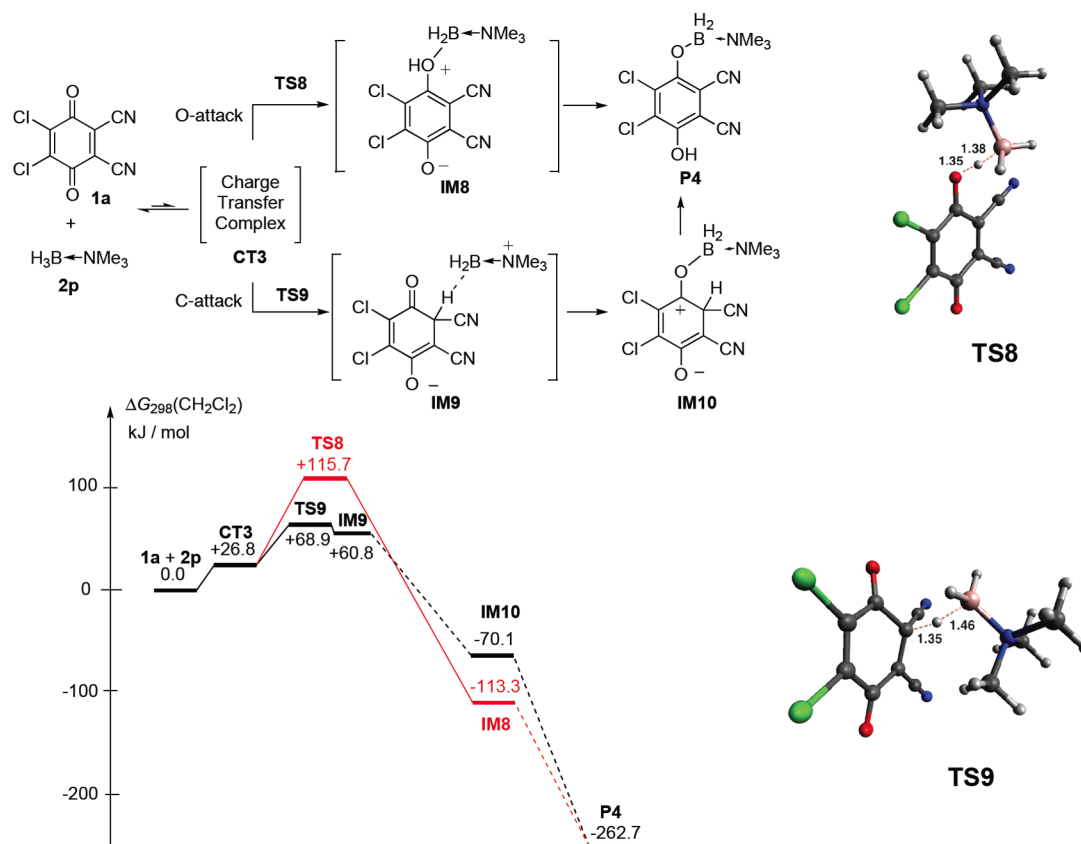
Figure 8. Free energy profile for the reaction of DDQ (**1a**) with trimethylamine–borane (**2p**) (RM06-2X/def2-TZVPP//B97D/6-31+G(d,p)//PCM/UFF) in CH$_2$Cl$_2$ together with selected transition structures.

Table 4. Rate Constants Derived from Activation Gibbs Free Energies (RM06-2X/def2-TZVPP//B97D/6-31+G(d,p)//PCM/UFF) for O-Attack and C-Attack Pathways of Reactions of DDQ with 2 in CH$_2$Cl$_2$ at 25 °C and Experimental Values in CH$_2$Cl$_2$ at 20 °C

	log $(k_2/M^{-1}\ s^{-1})$ RM06-2X, 25 °C		log $(k_2/M^{-1}\ s^{-1})$ exptl, 20 °C
nucleophile	O attack[a]	C attack[a]	
2a	−4.79 (8)	−7.50 (8)	−3.28
2b	−4.54 (4)	−6.49 (4)	−2.66
2c	−4.47 (4)	−4.60 (4)	−2.12
2d	0.38 (8)	−2.00 (8)	0.34
2e	−0.35 (16)	−3.21 (16)	−0.31
2f	2.86 (16)	−0.23 (16)	2.04
2g	3.67 (4)	2.43 (4)	3.08
2h	5.15 (16)	2.08 (16)	4.77
2j	0.28 (8)	−3.02 (8)	0.82
Bu$_3$SnH (**2n**)			2.79
Me$_3$SnH (**2n′**)	−4.67 (4)	2.62 (4)	2.10[b]
2p	−6.40 (12)	1.80 (12)	0.49
2q	−5.98 (12)	3.01 (12)	2.23
2r	−1.98 (12)	6.27 (12)	3.71
2t	−0.25 (12)	6.83 (12)	4.23

[a]Statistical factor in parentheses. [b]Calculated from the rate constant k_2 = 125 M^{-1} s^{-1} in CH$_3$CN at 25 °C reported in ref 22.

The deviation of the experimental rate constants for the reactions of DDQ (**1a**) with C−H hydride donors from those calculated from the reactivity parameters E, N, and s_N by eq 1
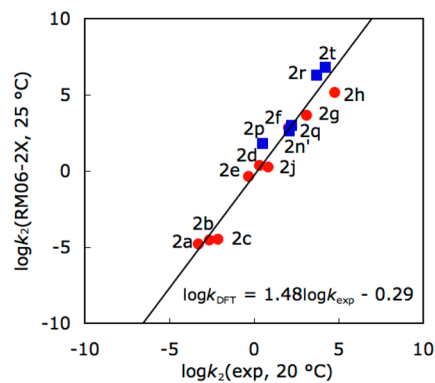

Figure 9. Correlation of quantum chemically calculated rate constants (log k_2(RM06-2X, 25 °C), from Table 4) for the reactions of DDQ (**1a**) with C−H hydride donors (O attack, red circles) and Sn−H and B−H hydride donors (C attack, blue squares) with the experimental values from Table 1.

was explained by the fact that the experimental data refer to transfer of H$^-$ to the quinone oxygen, while the E parameters of quinones refer to the quinone carbons, with the consequence that eq 1 calculates the transfer of H$^-$ to the quinone carbon atoms. For that reason we have compared the quantum chemically calculated rate constants for the nonobserved transfer of hydride from C−H to C-5 of DDQ (**1a**) with the corresponding rate constants obtained from the linear free energy relationship (eq 1). Figure 10 shows a remarkably good agreement of the absolute rate constants obtained by two completely different approaches. The applicability of eq 1 also
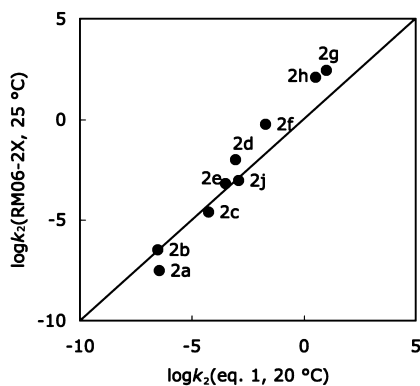
Figure 10. Rate constants for the nonobserved reactions of C−H hydride donors with C-5 of DDQ (**1a**): comparison of quantum chemically calculated rate constants (log k_2(RM06-2X, 25 °C), from Table 4) with the log k_2(20 °C) values derived from eq 1, by using the electrophilicity parameter E(**1a**) = −3.66 and the N and s_N parameters from Table 1.

for hydride transfer reactions from C−H hydride donors to quinones has thus been demonstrated.

The calculated energy profiles also provide an explanation for the largely differing kinetic isotope effects for the different systems. From the reaction profile shown in Figure 6 for the reaction of DDQ (**1a**) with cyclohexadiene (**2e**) we can see that the lowest-lying transition state **TS1** describes the exothermic/exergonic conversion of reactant complex **CT1** to ion pair **IM1**. This is not so for the reaction of DDQ (**1a**) with stannane **2n′**, where the lowest-lying transition state **TS7** characterizes the endergonic formation of ion pair **IM6** from reactant complex **CT2** (Figure 7). Similar observations can also be made for the borane reduction reaction in Figure 8, and we therefore believe that the rather small KIE values for reactions of stannanes and boranes indicate systematically later transition states connected to the formation of energetically high lying ion pair intermediates.

CONCLUSION

Correlation eq 1, which has previously been demonstrated to hold for a large variety of reactions of carbocations and Michael acceptors with π, n, and σ nucleophiles, has now been demonstrated also to hold for the reactions of quinones with Sn−H and B−H hydride donors, but not for the corresponding reactions with C−H hydride donors. The contrasting behavior of the different hydride donors turned out to be due to the fact that Sn−H and B−H groups transfer hydrogen to the conjugate carbons of the investigated quinones, while C−H hydride donors transfer hydrogen to the carbonyl oxygens. This conclusion is supported by deuterium labeling experiments and quantum chemical intrinsic reaction coordinate calculations.

Figures 6−8 show that the hydride transfer step from 1,4-cyclohexadiene to the DDQ oxygen is exergonic, resulting in large kinetic isotope effects (k_H/k_D = 6−9). In the reactions of DDQ with B−H and Sn−H hydride donors, on the other hand, the rate-determining hydride transfers to C-5 of DDQ lead to high-energy intermediates with late, product-like transition states, resulting in small and even inverse H/D kinetic isotope effects because of the smaller stretching force constants of B−H and Sn−H bonds in comparison to C−H bonds.

The electrophilicity parameters E of quinones, which have been derived from their reactivities toward π_{CC} nucleophiles,[5]

can be combined with the benzhydrylium-derived N and s_N parameters of Sn−H and B−H hydride donors to calculate the rate constants for the reactions of quinones with these hydride donors. The analogy of the involved mechanisms is thus demonstrated. The polar nature of these processes is further supported by the higher reactivity of Bu$_3$SnH in comparison to Ph$_3$SnH, which would not be the case if the Sn−H bond would be cleaved homolytically.[11]

As the E parameters of electrophiles are based on their reactivities toward C-centered reference nucleophiles, and the N and s_N parameters of nucleophiles are based on their reactivities toward C-centered reference electrophiles (typically benzhydrylium ions and quinone methides), the applicability of eq 1 is limited to electrophile−nucleophile combinations, in which at least one of the reaction centers is carbon. Since this condition is not fulfilled for the hydride shift from C−H groups to the carbonyl oxygen of quinones (formation of an O−H bond), the failure of eq 1 to reproduce the rate constants for this reaction series can be rationalized. Figure 10 shows, however, that eq 1 accurately predicts the quantum chemically derived rate constants for the nonobserved transfer of hydride from C−H groups to C-5 of DDQ (**1a**).

EXPERIMENTAL SECTION

Materials. The cyclohexa-1,4-diene derivatives **2f−h** were synthesized by Birch reduction according to a literature procedure.[23] **2i** was prepared through reduction of 4,4′-dimethoxybenzophenone with triethylsilane in the presence of HBF$_4$. **2k,l** were synthesized by reduction of the corresponding acridinium and pyridinium salts with NaS$_2$O$_4$ according to refs 24 and 25. **2s,t** were prepared by deprotonation of their carbene precursors and treated with THF−borane complex according to literature procedures.[26] D$_8$-1,4-cyclohexadiene was prepared by Birch reduction of D$_6$-benzene in liquid deuterated ammonia according to ref 27. Bu$_3$SnD was synthesized from the reaction of tributyltin chloride with LiAlD$_4$. The pyridine·BD$_3$ complex was obtained in pyridine solution by treatment of NaBD$_4$ with pyridine deuterium chloride, which was prepared from the deuterium exchange of pyridine hydrogen chloride with heavy water. **1b** was prepared by chlorination and subsequent oxidation of 1,4-dimethoxybenzene as reported in the literature.[28] All other compounds were purchased from commercial sources and (if necessary) purified by crystallization, sublimation (for benzoquinone), or distillation prior to use.

Kinetics. Dichloromethane was freshly distilled over CaH$_2$ before use. Commercially available cyclohexane, n-Bu$_2$O, and THF were further purified by distillation over DDQ to remove the impurities which may react with DDQ. Acetone and acetonitrile were purchased from Acros and used without further purification. Most rate constants were determined photometrically as described previously. Fast reactions were determined by using the stopped-flow technique. Slow reactions were measured by UV−vis (conventional photodiode array) or ^{1}H NMR spectroscopy (200 MHz, in CD$_3$CN) under nitrogen.[29] The temperature of the solutions during all kinetic studies was kept constant (20.0 ± 0.1 °C) by using a circulating bath thermostat.

ASSOCIATED CONTENT

Ⓢ Supporting Information

Text, figures, and tables giving details of the kinetic experiments and quantum chemical calculations. This material is available free of charge via the Internet at http://pubs.acs.org.

AUTHOR INFORMATION

Corresponding Author
*herbert.mayr@cup.uni-muenchen.de

■ REFERENCES

(1) (a) Becker, H.-D. In *The Chemistry of the Quinoid Compounds, Part I*; Patai, S., Ed.; Wiley: Chichester, U.K., 1974; pp 335–423. (b) Becker, H.-D.; Turner, A. B. In *The Chemistry of the Quinoid Compounds Vol. 2*; Patai, S., Rappoport, Z., Eds.; Wiley: Chichester, U.K., 1988; pp 1351–1384.

(2) (a) *Cytochrome P450: Structure, Mechanism, and Biochemistry*, 3rd ed.; Ortiz de Montellano, P. R., Ed.; Kluwer Academic/Plenum Publishers: New York, 2005. (b) Lai, W.; Li, C.; Chen, H.; Shaik, S. *Angew. Chem., Int. Ed.* **2012**, *51*, 5556–5578. (c) Shaik, S.; Cohen, S.; Wang, Y.; Chen, H.; Kumar, D.; Thiel, W. *Chem. Rev.* **2010**, *110*, 949–1017.

(3) (a) Trost, B. M. *J. Am. Chem. Soc.* **1967**, *89*, 1847–1851. (b) Müller, P.; Roček, J. *J. Am. Chem. Soc.* **1972**, *94*, 2716–2719. (c) Stoos, F.; Roček, J. *J. Am. Chem. Soc.* **1972**, *94*, 2719–2723. (d) Thummel, R. P.; Cravey, W. E.; Cantu, D. B. *J. Org. Chem.* **1980**, *45*, 1633–1637. (e) Müller, P. *Helv. Chim. Acta* **1973**, *56*, 1243–1251. (f) Müller, P.; Joly, D. *Helv. Chim. Acta* **1983**, *66*, 1110–1118. (g) Carlson, B. W.; Miller, L. L. *J. Am. Chem. Soc.* **1985**, *107*, 479–485. (h) Paukstat, R.; Brock, M.; Heesing, A. *Chem. Ber.* **1985**, *118*, 2579–2592. (i) Brock, M.; Hintze, H.; Heesing, A. *Chem. Ber.* **1986**, *119*, 3727–3736. (j) Fukuzumi, S.; Koumitsu, S.; Hironaka, K.; Tanaka, T. *J. Am. Chem. Soc.* **1987**, *109*, 305–316. (k) Zaman, K. M.; Yamamoto, S.; Nishimura, N.; Maruta, J.; Fukuzumi, S. *J. Am. Chem. Soc.* **1994**, *116*, 12099–12100. (l) Rüchardt, C.; Gerst, M.; Ebenhoch, J. *Angew. Chem., Int. Ed. Engl.* **1997**, *36*, 1406–1430. (m) Höfler, C.; Rüchardt, C. *Liebigs Ann. Chem.* **1996**, 183–188. (n) Wurche, F.; Sicking, W.; Sustmann, R.; Klärner, F.-G.; Rüchardt, C. *Chem. Eur. J.* **2004**, *10*, 2707–2721. (o) Chan, B.; Radom, L. *J. Phys. Chem. A* **2007**, *111*, 6456–6467. (p) Batista, V. S.; Crabtree, R. H.; Konezny, S. J.; Luca, O. R.; Praetorius, J. M. *New J. Chem.* **2012**, *36*, 1141–1144.

(4) For the series of papers, see: (a) Braude, E. A.; Jackman, L. M.; Linstead, R. P. *J. Chem. Soc.* **1954**, 3548–3563. (b) Braude, E. A.; Jackman, L. M.; Linstead, R. P. *J. Chem. Soc.* **1954**, 3564–3568. (c) Braude, E. A.; Brook, A. G.; Linstead, R. P. *J. Chem. Soc.* **1954**, 3569–3574. (d) Braude, E. A.; Linstead, R. P.; Wooldridge, K. R. *J. Chem. Soc.* **1956**, 3070–3074. (e) Barnard, J. R.; Jackman, L. M. *J. Chem. Soc.* **1960**, 3110–3115. (f) Braude, E. A.; Jackman, L. M.; Linstead, R. P.; Shannon, J. S. *J. Chem. Soc.* **1960**, 3116–3122. (g) Braude, E. A.; Jackman, L. M.; Linstead, R. P.; Lowe, G. *J. Chem. Soc.* **1960**, 3123–3132. (h) Braude, E. A.; Jackman, L. M.; Linstead, R. P.; Lowe, G. *J. Chem. Soc.* **1960**, 3133–3138. For a review, see: (i) Jackman, L. M. In *Advances in Organic Chemistry, Methods and Results Vol. 2*; Raphael, R. A., Taylor, E. C., Wynberg, H., Eds.; Interscience: New York, 1960.

(5) (a) Guo, X.; Mayr, H. *J. Am. Chem. Soc.* **2013**, *135*, 12377–12387. (b) Guo, X.; Mayr, H. *J. Am. Chem. Soc.* **2014**, *136*, 11499–11512.

(6) (a) Thiele, J.; Günther, F. *Liebigs Ann. Chem.* **1906**, *349*, 45–66. (b) Walker, D.; Hiebert, J. D. *Chem. Rev.* **1967**, *67*, 153–195. (c) Buckle, D. R. In *Encyclopedia of Reagents for Organic Synthesis Vol. 3*; Paquette, L. A., Ed.; Wiley: Chichester, U.K., 1995; p 1699.

(7) (a) Zhang, Y.; Li, C. J. *Angew. Chem., Int. Ed.* **2006**, *45*, 1949–1952. (b) Zhang, Y.; Li, C. J. *J. Am. Chem. Soc.* **2006**, *128*, 4242–4243. (c) Tu, W.; Floreancig, P. E. *Angew. Chem., Int. Ed.* **2009**, *48*, 4567–4571. (d) Liu, L.; Floreancig, P. E. *Angew. Chem., Int. Ed.* **2010**, *49*, 3069–3072. (e) Guo, C.; Song, J.; Luo, S. W.; Gong, L. Z. *Angew.* *Chem., Int. Ed.* **2010**, *49*, 5558–5562. (f) Hayashi, Y.; Itoh, T.; Ishikawa, H. *Angew. Chem., Int. Ed.* **2011**, *50*, 3920–3924. (g) Tsang, A. S.-K.; Jensen, P.; Hook, J. M.; Hashmi, A. S. K.; Todd, M. H. *Pure Appl. Chem.* **2011**, *83*, 655–665. (h) Alagiri, K.; Devadig, P.; Prabhu, K. R. *Chem. Eur. J.* **2012**, *18*, 5160–5164. (i) Rohlmann, R.; Garcia Mancheño, O. *Synlett* **2013**, *24*, 6–10. (j) Singh, K. N.; Singh, P.; Singh, P.; Maheshwary, Y.; Kessar, S. V.; Batra, A. *Synlett* **2013**, *24*, 1963–1967.

(8) (a) Mayr, H.; Patz, M. *Angew. Chem., Int. Ed. Engl.* **1994**, *33*, 938–957. (b) Mayr, H.; Ofial, A. R. *Pure Appl. Chem.* **2005**, *77*, 1807–1821. (c) Mayr, H.; Ofial, A. R. *J. Phys. Org. Chem.* **2008**, *21*, 584–595. (d) Mayr, H.; Kempf, B.; Ofial, A. R. *Acc. Chem. Res.* **2003**, *36*, 66–77.

(9) For a comprehensive database of nucleophilicity parameters N and s_N as well as electrophilicity parameters E, see http://www.cup.lmu.de/oc/mayr/DBintro.html.

(10) Horn, M.; Schappele, L. H.; Lang-Wittkowski, G.; Mayr, H.; Ofial, A. R. *Chem. Eur. J.* **2013**, *19*, 249–263.

(11) Carlsson, D. J.; Ingold, K. U. *J. Am. Chem. Soc.* **1968**, *90*, 7047–7055.

(12) (a) Reichardt, C. *Angew. Chem., Int. Ed. Engl.* **1979**, *18*, 98–110. (b) Reichardt, C.; Welton, T. *Solvents and Solvent Effects in Organic Chemistry*, 4th ed.; Wiley-VCH: Weinheim, Germany, 2010.

(13) Heyes, D.; Menon, R. S.; Watt, C. I. F.; Wiseman, J.; Kubinski, P. *J. Phys. Org. Chem.* **2002**, *15*, 689–700.

(14) (a) Wigfield, D. C.; Phelps, D. J. *Can. J. Chem.* **1972**, *50*, 388–394. (b) Wigfield, D. C.; Gowland, F. W. *Tetrahedron Lett.* **1979**, 2209–2212. (c) Yamataka, H.; Hanafusa, T. *J. Am. Chem. Soc.* **1986**, *108*, 6643–6646.

(15) Mayr, H.; Bug, T.; Gotta, M. F.; Hering, N.; Irrgang, B.; Janker, B.; Kempf, B.; Loos, R.; Ofial, A. R.; Remennikov, G.; Schimmel, H. *J. Am. Chem. Soc.* **2001**, *123*, 9500–9512.

(16) Davis, R. E.; Brown, A. E.; Hopmann, R.; Kibby, C. L. *J. Am. Chem. Soc.* **1963**, *85*, 487.

(17) Colter and co-workers have previously reported that no excess deuterium was observed in the hydroquinone isolated from the reaction of 9-deuterated *N*-methylacridan with benzoquinone, which supports the O-attack mechanism. Colter, A. K.; Saito, G.; Sharom, F. J. *Can. J. Chem.* **1977**, *55*, 2741–2751.

(18) Frisch, M. J.; Trucks, G. W.; Schlegel, H.; Scuseria, G. E.; Robb, M. A.; Cheeseman, J. R.; Scalmani, G.; Barone, V.; Mennucci, B.; Petersson, G. A.; Nakatsuji, H.; Caricato, M.; Li, X.; Hratchian, H. P.; Izmaylov, A. F.; Bloino, J.; Zheng, G.; Sonnenberg, J. L.; Hada, M.; Ehara, M.; Toyota, K.; Fukuda, R.; Hasegawa, J.; Ishida, M.; Nakajima, T.; Honda, Y.; Kitao, O.; Nakai, H.; Vreven, T.; Montgomery, J. A.; Peralta, J. E.; Ogliaro, F.; Bearpark, M.; Heyd, J. J.; Brothers, E.; Kudin, K. N.; Staroverov, V. N.; Kobayashi, R.; Normand, J.; Raghavachari, K.; Rendell, A.; Burant, J. C.; Iyengar, S. S.; Tomasi, J.; Cossi, M.; Rega, N.; Millam, J. M.; Klene, M.; Knox, J. E.; Cross, J. B.; Bakken, V.; Adamo, C.; Jaramillo, J.; Gomperts, R.; Stratmann, R. E.; Yazyev, O.; Austin, A. J.; Cammi, R.; Pomelli, C.; Ochterski, J. W.; Martin, R. L.; Morokuma, K.; Zakrzewski, V. G.; Voth, G. A.; Salvador, P.; Dannenberg, J. J.; Dapprich, S.; Daniels, A. D.; Farkas; Foresman, J. B.; Ortiz, J. V.; Cioslowski, J.; Fox, D. J. *Gaussian 09, Revision A.02*; Gaussian, Inc., Wallingford, CT, 2009.

(19) Marenich, A. V.; Cramer, C. J.; Truhlar, D. G. *J. Phys. Chem. B* **2009**, *113*, 6378–6396.

(20) For **2c**, similar rates for O and C attack were calculated.

(21) (a) Nagase, S.; Morokuma, K. *J. Am. Chem. Soc.* **1978**, *100*, 1666–1672. (b) Ess, D. H.; Houk, K. N. *J. Am. Chem. Soc.* **2007**, *129*, 10646–10647. (c) Ess, D. H.; Houk, K. N. *J. Am. Chem. Soc.* **2008**, *130*, 10187–10198. (d) Ess, D. H.; Jones, G. O.; Houk, K. N. *Org. Lett.* **2008**, *10*, 1633–1636. (e) Bickelhaupt, F. M. *J. Comput. Chem.* **1999**, *20*, 114–128. (f) Diefenbach, A.; Bickelhaupt, F. M. *J. Chem. Phys.* **2001**, *115*, 4030–4040. (g) Diefenbach, A.; Bickelhaupt, F. M. *J. Phys. Chem. A* **2004**, *108*, 8460–8466.

(22) Klingler, R. J.; Mochida, K.; Kochi, J. K. *J. Am. Chem. Soc.* **1979**, *101*, 6626–6637.

(23) Krapcho, A. P.; Bothner-By, A. A. *J. Am. Chem. Soc.* **1959**, *81*, 3658–3666.

(24) Roberts, R. M. G.; Ostovic, D.; Kreevoy, M. M. *Faraday Discuss. Chem. Soc.* **1982**, *74*, 257−265.

(25) Mauserall, D.; Westheimer, F. H. *J. Am. Chem. Soc.* **1955**, *77*, 2261−2264.

(26) (a) Ueng, S.-H.; Makhlouf Brahmi, M.; Derat, E.; Fensterbank, L.; Lacôte, E.; Malacria, M.; Curran, D. P. *J. Am. Chem. Soc.* **2008**, *130*, 10082−10083. (b) Walton, J. C.; Makhlouf Brahmi, M.; Fensterbank, L.; Lacôte, E.; Malacria, M.; Chu, Q.; Ueng, S.-H.; Solovyev, A.; Curran, D. P. *J. Am. Chem. Soc.* **2010**, *132*, 2350−2358.

(27) Cowley, R. E.; Eckert, N. A.; Vaddadi, S.; Figg, T. M.; Cundari, T. R.; Holland, P. L. *J. Am. Chem. Soc.* **2011**, *133*, 9796−9811.

(28) López-Alvarado, P.; Avendaño, C.; Menéndez, J. C. *Synth. Commun.* **2002**, *32*, 3233−3239.

(29) For the slow reactions with tributylstannane, contact with oxygen should be avoided, because it might initiate radical chain reactions. For general principles of radical chain reactions of stannanes, see: Zard, S. Z. *Radical Reactions in Organic Synthesis*; Oxford University Press: New York, 2003.

(30) One reviewer, though agreeing with our conclusions, missed a simple chemical rationale for the different behaviors of the C−H hydride donors on one side and B−H and Sn−H on the other. We regret that we cannot provide such a rationale, but instead of presenting an ostensible explanation, we prefer to follow the advice of our senior colleague Rolf Huisgen: "Do not detract the excitement of mystery from unsolved problems."